

Lightweight design optimization of a welded monorail track using an evolutionary algorithm

Goran V. Pavlović^{1*}, Mile M. Savković¹, Vanio Ralev², Spasoje Trifković³, Predrag Z. Mladenović¹

¹ University of Kragujevac, Faculty of Mechanical and Civil Engineering, Kraljevo, Serbia

² Todor Kableshkov University of transport (VTU), Sofia, Bulgaria

³ University of East Sarajevo, Faculty of Mechanical Engineering, Sarajevo, Bosnia and Herzegovina

ARTICLE INFO

*Correspondence: goranthejavovic@yahoo.com

DOI: 10.5937/engtoday2600003P

UDC: 621(497.11)

ISSN: 2812-9474

Article history: Received 12 January 2026; Revised 30 January 2026; Accepted 3 February 2026

ABSTRACT

This study presents the analysis and optimization of the mass of monorail track girders. Two types of girders were considered: a mono-symmetric welded I-profile and a double-symmetric I-profile variant. The objective function was the cross-sectional area of the I-profile, including weld areas. Constraints included the strength at critical points of the I-profile, weld strength, girder stiffness, and overall stability. The monorail track was analyzed in the span between two supports. An Evolutionary Algorithm, implemented in the Solver add-in of MS Excel, was used for optimization, allowing discrete design variables such as standard plate thicknesses and integer weld dimensions, thereby providing practical and implementable solutions. The proposed model was applied to real monorail tracks in operation that utilize standard I-profiles. The optimized solutions demonstrated material savings while satisfying all limit criteria, confirming the efficiency and applicability of the approach for practical design improvements in monorail track construction.

KEYWORDS

Evolutionary Algorithm, Design optimization, Welded beam, Monorail crane, Spreadsheet-based optimization.

1. INTRODUCTION

Monorail crane systems, in addition to single-girder and double-girder bridge cranes, are widely used in various types of industrial facilities and manufacturing plants, especially in applications where heavy loads are not involved, as well as in situations where space limitations or specific transport paths prevent the use of conventional overhead cranes. Structurally, monorail cranes consist primarily of a single beam or truss system subjected to concentrated moving loads. Therefore, strength, stiffness, and structural stability of the monorail beam are critical design aspects, particularly with respect to bending resistance, deflection limits, and buckling behavior.

For this purpose, various types of standard I-profile beams are most commonly used. However, because the I-profile is subjected to a specific type of loading in these cases, its geometry often results in the monorail track being over-designed, meaning the profile is not used in a structurally efficient manner. For this reason, it is more rational to use a welded girder, which is the focus of the present study.

The structural integrity of monorail crane systems is fundamentally dependent on the strength of the girder and its resistance to stability failures such as buckling and excessive deformation. Because monorail systems consist of a

single beam supporting moving loads from a hanging trolley, the structural design must ensure both sufficient carrying capacity and resistance to instability phenomena, particularly lateral-torsional buckling. Due to the prevalence of this type of girder in practice, there are numerous publications that address this topic, primarily with regard to strength and stability.

The paper [1] presents one of the foundational studies on monorail stability where investigated the lateral-torsional buckling behavior of overhanging monorail beams. Detailed Finite Element Analysis (FEA) demonstrated that the location of applied loads and support conditions significantly influence the buckling capacity of the beam. The research also quantified how cross-section distortion reduces buckling resistance, and provided practical recommendations to improve design against lateral instability. Similarly, [2] shows elastic lateral-distortional buckling of overhanging monorail I-beams significantly reduces buckling resistance compared to flexural-torsional modes, depending on web slenderness and support restraints, with FEA used to quantify critical design parameters. The author of the previous work in the paper [3] investigates the elastic lateral-distortional buckling of overhanging monorail I-beams, demonstrating that distortion of the slender web significantly reduces the elastic buckling resistance below the flexural-torsional resistance, with FEA used to quantify how section geometry, support restraints, and overhang length influence critical buckling loads. The review paper [4] of monorail crane design literature summarize the unique structural issues related to monorail systems, including the effects of moving loads, minor axis bending, and torsional loading, particularly for curved beams. These reviews emphasize that monorail structural design must address buckling phenomena and deformation behavior specific to I-section beams, and that addressing such issues is essential for ensuring the structural performance and serviceability of the monorail system.

Structural performance analyses of specific monorail crane configurations provide insight into static strength and serviceability. For example, a frame analysis of an 8-ton capacity monorail crane using Autodesk Inventor simulation examined bending moments, shear forces, normal stresses, and displacements under rated load, [5]. The results indicated that maximum stresses and deflections remained within allowable limits for the selected structural material and design, confirming adequate strength and structural suitability for service loads.

In addition to the use of FEA, many analytical methods are also frequently employed, as well as the application of optimization procedures. Although a wide range of metaheuristic algorithms have gained significant popularity for engineering problems, and their applications in numerous engineering examples have been demonstrated in [6]. Ms Excel also has very practical use. It can be successfully applied to various nonlinear optimization problems by using the Generalized Reduced Gradient (GRG2) algorithm or the Evolutionary Algorithm (EA), as shown in studies [7, 8] on examples of crane carrying structures.

The aim of this research is to optimize the geometric parameters of the welded I-girder of a monorail crane in order to obtain a structurally efficient design with the minimum possible girder mass. For this reason, the welded I-girder structure has been proposed, where the goal is to reduce the cross-sectional area of I-profile. This necessitates a detailed analysis of the loading on the monorail beam. Also, for practical reasons, it is planned to use standard plate thicknesses, with certain variables taking those values during the optimization process. For this reason, Ms Excel was chosen, with the EA providing the capability to perform this type of optimization. Two monorail crane examples will be used as case studies.

2. ANALYSIS AND OPTIMIZATION PROBLEM

In this study, the analysis and optimization of the cross-section of the monorail track between two supports (considered as a simply supported beam) are examined. A welded I-girder was adopted for the monorail track, with the crane load applied at the mid-span between the two supports as a concentrated force. The specific weight of the girder was also taken into account. The goal is to minimize the cross-sectional area of the girder while satisfying all design requirements applicable to such carrying structures. The main goal, therefore, is the optimal determination of the geometric dimensions of the I-section, in order to achieve a rationally utilized I-section while fulfilling all necessary criteria.

2.1. The objective function, input parameters and optimization variables

The objective function in this study is the cross-sectional area of I-girder (Figure 2). All necessary parameters and variables are shown in Figures 1 and 2. Input parameters necessary for this optimization problem are:

$$Q, L, m_t, n_t, b_m, h_m, A_{pr}, \rho_m, R_e, E \quad (1)$$

where Q is the carrying capacity, L is the mid-span between two supports, m_t is the trolley mass, n_t is the number of trolley wheels, b_m, h_m are the minimum required dimensions of the I-section for the installation of the crane on the monorail track for the width and height of I-profile, respectively, A_{pr} is the cross-sectional area of standard I-profile, ρ_m is the material density of plates, R_e is the yield strength of plates, [9], and E is Young's modulus of plates.

The optimization variables (Figure 2) are:

$$b_1, t_1, b_2, t_2, h, s, a_w \quad (2)$$

where b_1, t_1, b_2, t_2, s are dimensions of the plates of I-section, and a_w is the weld thickness.

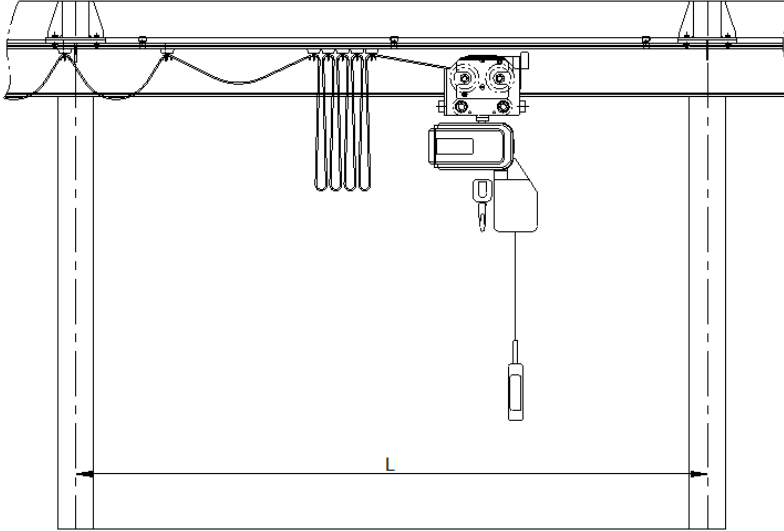


Figure 1: The layout of a monorail crane system

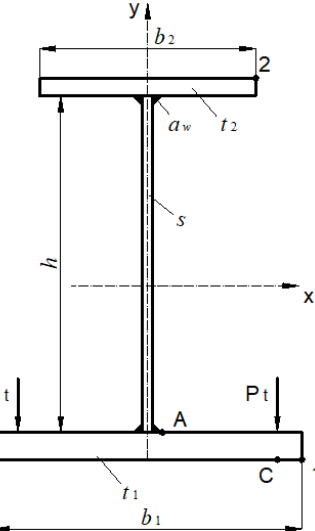


Figure 2: The cross-section of I-girder

The cross-sectional area (A_m) of the welded monorail track (I-section) is shown on Figure 2. The cross-sectional area (the objective function) is defined in the following way:

$$A_m = b_1 \cdot t_1 + b_2 \cdot t_2 + h \cdot s + 4 \cdot a_w^2 \quad (3)$$

The geometric characteristics of I-section (Figure 2) are: W_{px} – the section moduli for point p ($p = 1, 2, A, C$) about x-axis, I_x, I_y – the principal moments of inertia about x and y-axis, respectively, S_x – the static moment of inertia, and I_D – the torsional moment of inertia. These geometric characteristics in the continuation of this paper are being calculated by using the well-known expressions for the used cross section.

2.2. The constraints

The monorail track must satisfy strength requirements for both the profile material and the welded joints, as well as stability criteria, mid-span deflection between two supports, and geometric constraints related to the installation of the crane on the I-girder (rail). The verification of strength, stability, and deflection is performed according to the procedure presented in [9-13]. In the following, all relevant quantities required for the calculations are presented:

$$F_v = \gamma \cdot (\psi \cdot Q + m_t) \cdot g \quad (4)$$

$$M_v = \frac{F_v}{4} \cdot L + \gamma \cdot \frac{q \cdot L^2}{8} \quad (5)$$

$$q = \rho_m \cdot g \cdot A_m \quad (6)$$

$$F_{st} = (Q + m_t) \cdot g \quad (7)$$

$$P_t = \frac{F_v}{n_t} \quad (8)$$

$$F_T = F_v + \gamma \cdot \frac{q \cdot L}{2} \quad (9)$$

where F_v is the maximum force from the trolley in the vertical plane, F_{st} is the maximum static force in the vertical plane, F_T is the maximum shear force in the vertical plane, P_t is the maximum force in the vertical plane from the trolley wheel (the maximum pressure of the trolley wheel), M_v is the maximum bending moment in the vertical plane, q is the specific weight per unit of length of the girder, g is the acceleration due to gravity, γ is the coefficient (depends on the Classification class, [10]), and ψ is the dynamic coefficient of the influence of load oscillation in the vertical plane, [10].

The strength at specific points of the I-section is calculated using the following expressions, and the following condition must be satisfied:

$$\sigma_A = \sqrt{(\sigma_{Az} + \sigma_{Akz})^2 + \sigma_{Akx}^2} - (\sigma_{Az} + \sigma_{Akz})\sigma_{Akx} \leq \sigma_{p1} \quad (10)$$

$$\sigma_{Az} = \frac{M_v}{W_{Ax}} \quad (11)$$

$$\sigma_{Akz} = K_{Az} \cdot \frac{P_t}{t_1^2} \quad (12)$$

$$\sigma_{Akx} = K_{Ax} \cdot \frac{P_t}{t_1^2} \quad (13)$$

$$\sigma_{p1} = \frac{R_e}{V_1}, \quad V_1 = 1.5 \quad (14)$$

$$\sigma_C = \sqrt{(\sigma_{Cz} + \sigma_{Ckz})^2 + \sigma_{Ckx}^2} - (\sigma_{Cz} + \sigma_{Ckz})\sigma_{Ckx} \leq \sigma_{p2} \quad (15)$$

$$\sigma_{Cz} = \frac{M_v}{W_{Cx}} \quad (16)$$

$$\sigma_{Ckz} = K_{Cz} \cdot \frac{P_t}{t_1^2} \quad (17)$$

$$\sigma_{Ckx} = K_{Cx} \cdot \frac{P_t}{t_1^2} \quad (18)$$

$$\sigma_{p2} = \frac{R_e}{V_2}, \quad V_2 = 1.33 \quad (19)$$

$$\sigma_1 = \frac{M_v}{W_{1x}} \leq \sigma_{p1} \quad (20)$$

$$\sigma_2 = \frac{M_v}{W_{2x}} \leq \sigma_{p1} \quad (21)$$

where: σ_p is the total stress in the observed point p ($p = 1, 2, A, C$), σ_{Az}, σ_{Cz} are the normal stresses in the points A and C, respectively, $\sigma_{Akz}, \sigma_{Akx}$ are local stresses in point A, in both directions, respectively, $\sigma_{Ckz}, \sigma_{Ckx}$ are local stresses in point C, in both directions, respectively, K_{Az}, K_{Ax} are corresponding coefficients for local stresses in point A, respectively, [10], K_{Cz}, K_{Cx} are corresponding coefficients for local stresses in point C, respectively, [10], V_1, V_2 are the load factored coefficient for load cases 1 and 2, respectively, [9], and σ_{p1}, σ_{p2} are permissible stresses for load cases 1 and 2, respectively.

The strength of the welded joint is verified in the following manner, where the maximum weld stress (σ_w) must be lower than the permissible stress (σ_{wp}):

$$\sigma_w = \frac{F_T \cdot S_x}{2 \cdot I_x \cdot a_w} \leq \sigma_{wp} = 0.75 \cdot \sigma_{p1} \quad (22)$$

In addition, the weld size must satisfy (23):

$$a_w \leq 0.7 \cdot \min[s, \min(t_1, t_2)] \quad (23)$$

The stability of the girder is evaluated according to the procedure specified in standard [11]. It is verified whether the following condition is satisfied:

$$\frac{L}{i_y} \leq 40 \cdot \sqrt{\frac{23.5}{R_e}} \quad (24)$$

For S235 steel, which is considered in this study, based on (24), $i_y = L/40$ is obtained, and if this value exceeds i_p (the radius of gyration for the top flange of I-profile), a stability check is required. In that case, condition (25) must be fulfilled. The complete set of required relations is presented below:

$$\sigma_2 \leq \sigma_b = \frac{\sigma_D}{V_1} \quad (25)$$

$$\sigma_D = \alpha_p \cdot \chi_M \cdot R_e \leq R_e \quad (26)$$

$$\alpha_p = \frac{2 \cdot S_x}{W_{2x}} \quad (27)$$

$$\chi_M = \left(\frac{1}{1 + \overline{\lambda}_D^{-5}} \right)^{0.4} \quad (28)$$

$$\overline{\lambda}_D = \sqrt{\alpha_p \cdot \frac{R_e}{\sigma_{cr,D}}} \quad (29)$$

$$\sigma_{cr,D} = \phi \cdot \eta \cdot \sqrt{1.679 \cdot 10^5 \cdot \frac{I_D \cdot I_y}{(W_{2x} \cdot L)^2} + \sigma_{E,y}^2}, \eta = 1.45 \quad (30)$$

$$\phi = \frac{\rho + \sqrt{1 + 0.156 \cdot \frac{I_D}{I_y} \cdot \left(\frac{L}{h} \right)^2 + \rho^2}}{\sqrt{1 + 0.156 \cdot \frac{I_D}{I_y} \cdot \left(\frac{L}{h} \right)^2}}, \rho = 0.55 \quad (31)$$

$$\sigma_{E,y} = \frac{\pi^2 \cdot E}{\lambda_y^2} \quad (32)$$

$$\lambda_y = \frac{L}{i_p} \quad (33)$$

$$i_p = \sqrt{\frac{I_p}{A_p}} \quad (34)$$

$$A_p = b_2 \cdot t_2 \quad (35)$$

$$I_p = \frac{b_2^3 \cdot t_2}{12} \quad (36)$$

where i_y is the radius of gyration about y -axis A_p, I_p , are geometric characteristic for the top flange of I-profile, λ_y is the slenderness for the top flange of I-profile about y -axis, σ_b is the permissible stress for lateral buckling, σ_D is the limit stress for lateral buckling, [11], α_p is the plastic shape factor, [11], χ_M is the non-dimensional reduction factor for lateral buckling, [11], $\overline{\lambda}_D$ is the relative slenderness for lateral buckling, [11], $\sigma_{cr,D}$ is the ideal stress for lateral buckling, [11], $\sigma_{E,y}$ is the part of the ideal stress [11], and η, ϕ, ρ , are non-dimensional parameters, [11].

The stability of the top (compressed) flange can also be verified using the provisions of standards [11-13]:

$$\sigma_2 \leq \sigma_{cr} = 1.14 \cdot \sigma_{i,p} \quad (37)$$

$$\sigma_{i,p} = \chi_p \cdot \sigma_{p1} \quad (38)$$

$$\chi_p = \frac{2}{\beta_v + \sqrt{\beta_v^2 - 4 \cdot \bar{\lambda}^2}}, \bar{\lambda} > 0.2 \quad (39)$$

$$\chi_p = 1, \bar{\lambda} \leq 0.2$$

$$\beta_v = 1 + 0.489 \cdot (\bar{\lambda} - 0.2) + \bar{\lambda}^2 \quad (40)$$

$$\bar{\lambda} = \frac{\lambda}{\lambda_v} \quad (41)$$

$$\lambda_v = \pi \cdot \sqrt{\frac{E}{R_e}} \quad (42)$$

$$\lambda = \frac{l_i}{i_p} \quad (43)$$

$$l_i = \beta \cdot L, \beta = \sqrt{\frac{1}{3.18}} \quad (44)$$

where σ_c is the critical stress, [11], $\sigma_{i,p}$ is the permissible buckling stress, χ_p is the non-dimensional reduction factor, β_v is non-dimensional value, [12], λ is the slenderness for the girder, [12], $\bar{\lambda}$ is the relative slenderness for the girder, [12], β is the non-dimensional girder slenderness, [13], l_i is the effective length, and λ_v is the yield slenderness, [12].

The maximum mid-span deflection (f_{max}) of the girder between two supports is calculated as follows:

$$f_{max} = \frac{F_{st} \cdot L^3}{48 \cdot I_x \cdot E} + \frac{5 \cdot q \cdot L^4}{384 \cdot I_x \cdot E} \leq f_p = K_f \cdot L \quad (45)$$

and its value must be lower than the permissible one (f_p),

where K_f is the stiffness coefficient (depends on Classification Class, [10]).

In addition to the above criteria, the following geometric constraints related to the installation of the crane on the I-section must be satisfied, where b_m denotes the minimum width of the bottom flange and h_m represents the minimum web height of the I-section, including an additional distance of 5 cm:

$$b_m \leq b_1 \quad (46)$$

$$h_m + 5 \leq h \quad (47)$$

Based on the expressions presented above, the following constraint functions are obtained:

$$g_1 = \sigma_1 - \sigma_{p1} \leq 0 \quad (48)$$

$$g_2 = \sigma_2 - \sigma_{p1} \leq 0 \quad (49)$$

$$g_3 = \sigma_A - \sigma_{p1} \leq 0 \quad (50)$$

$$g_4 = \sigma_C - \sigma_{p2} \leq 0 \quad (51)$$

$$g_5 = \sigma_w - 0.75 \cdot \sigma_{p1} \leq 0 \quad (52)$$

$$g_6 = a_w - 0.7 \cdot \min[s, \min(t_1, t_2)] \leq 0 \quad (53)$$

$$g_7 = \sigma_2 - \alpha_p \cdot \chi_M \cdot \frac{R_e}{V_1} \leq 0 \quad (54)$$

$$g_8 = \sigma_2 - 1.14 \cdot \chi_p \cdot \sigma_{p1} \leq 0 \quad (55)$$

$$g_9 = f_{max} - f_p \leq 0 \quad (56)$$

$$g_{10} = b_m - b_1 \leq 0 \quad (57)$$

$$g_{11} = h_m + 5 - h \leq 0 \quad (58)$$

where $g_i, i=1, \dots, 11$ are constraints functions.

3. OPTIMIZATION METHOD

An Evolutionary Algorithm (EA) was used in this study as the optimization method. EA in MS Excel (Solver add-in) is a heuristic optimization method inspired by the principles of natural selection. Solutions are iteratively improved through selection, crossover, and mutation, aiming to find a global optimum or a sufficiently good solution for non-linear and discontinuous problems.

The main reason for applying the EA within Ms Excel is its ability to handle optimization variables whose values are selected from predefined data sets, as is the case for plate thicknesses. The thickness values are selected from a specified range of standard plate thicknesses using the INDEX function in Ms Excel. In this way, unrealistic thickness values that would otherwise require subsequent rounding or manual adjustment are avoided. This approach results in a more realistic optimization model, making it suitable for practical engineering applications.

Figure 3 shows EA optimization parameters.

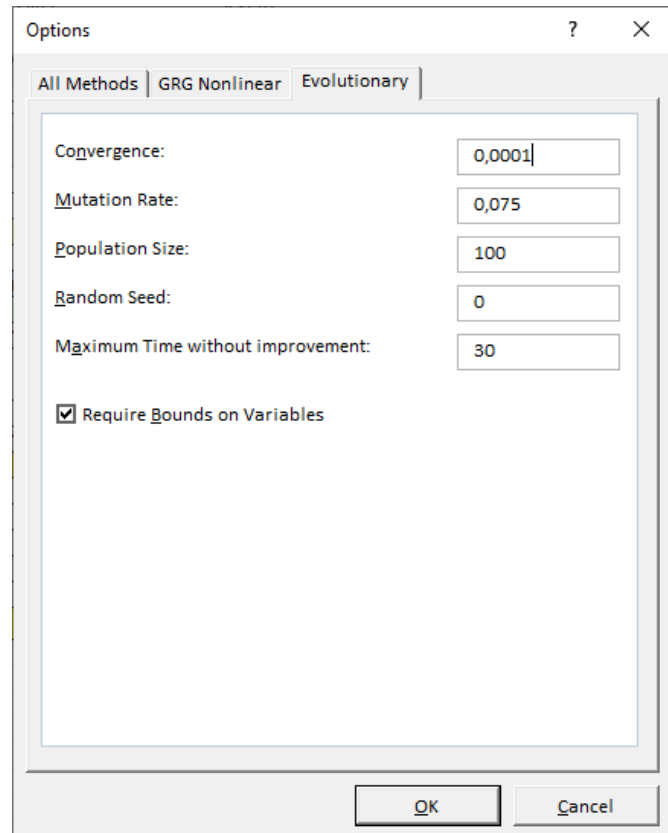


Figure 3: EA optimization parameters

4. RESULTS OF OPTIMIZATION AND DISCUSSION

The optimization procedure was carried out using the EA method implemented in Ms Excel, as presented in the previous section.

Table 1 provides the data for two monorail cranes currently in operation. The monorail track girders are standard I-beams made of S235 steel.

The objective function is defined by (3).

Constraints are defined by (47)-(58).

I-profiles are analyzed as the mono-symmetric I-profile (Variant 1, Figure 2) and the double-symmetric I-profile (Variant 2, $b_2 = b_1$, $t_2 = t_1$).

Table 1: Input parameters for monorail crane examples

	Q (t)	L (m)	Cl. Class	m_t (kg)	b_m (cm)	h_m (cm)	I-profile	A_{pr} (cm ²)
1	3.2	3.50	II	162	8.2	17.3	IPB-300	69.1
2	1	3.45	I	120	8.9	14.7	IPE-240	39.1

It was assumed that the widths of the top and bottom flanges do not exceed 300 mm, while, for Variant 1, the width of the top flange must not be less than 100 mm. The optimization variables are defined in (2). The following standard plate thicknesses (in millimeters) were considered:

- $s = [5, 6, 7, 8, 9, 10]$,

- $t_1 = [6, 7, 8, 9, 10, 12, 14, 15, 16, 18, 20, 22, 25, 28, 30, 35, 40]$,

- $t_2 = [6, 7, 8, 9, 10, 12, 14, 15, 16, 18, 20]$.

The following weld dimensions (in millimeters) were considered:

- $a_w = [3, 4, 5, 6, 7]$.

In addition to the data presented in Table 1, the following values were taken: $n_t = 4$, $\gamma = 1.0$, for Classification Class 1, and $\gamma = 1.05$, for Classification Class 2; $\psi = 1.15$; $K_f = 1/400$, for Classification Class 1, and $K_f = 1/500$, for Classification Class 2; the material of plates is S235 ($R_e = 23.5 \text{ kN/cm}^2$, $E = 21000 \text{ kN/cm}^2$, and $\rho_m = 7850 \text{ kg/m}^3$).

Due to the search mechanism of the EA during the optimization process and the stochastic nature of the obtained solutions, three simulations were performed for each examples and profile variant, and the best solution was taken.

Table 2: Optimization results for the mono-symmetric I-profile (Variant 1)

	h_{opt} (mm)	s_{opt} (mm)	$b_{1,\text{opt}}$ (mm)	$t_{1,\text{opt}}$ (mm)	$b_{2,\text{opt}}$ (mm)	$t_{2,\text{opt}}$ (mm)	$a_{w,\text{opt}}$ (mm)	$A_{m,\text{opt}}$ (cm^2)	Savings (%)
1	259.2	5	82	14	116	6	3	31.76	54.03
2	197	5	89	7	100	6	3	22.44	42.61

Table 3: Optimization results for the double-symmetric I-profile (Variant 2)

	h_{opt} (mm)	s_{opt} (mm)	$b_{1,\text{opt}}$ (mm)	$t_{1,\text{opt}}$ (mm)	$a_{w,\text{opt}}$ (mm)	$A_{m,\text{opt}}$ (cm^2)	Savings (%)
1	241.4	5	82	14	3	35.39	48.78
2	197	5	89	7	3	22.67	42.02

Table 2 presents the optimal values and material savings for Variant 1, for both examples, while Table 3 shows the optimal values and material savings for Variant 2, for both examples. A significant reduction in material consumption compared to the use of standard profiles can be observed (Tables 2 and 3).

Furthermore, based on the results presented in Tables 2 and 3, the influence of crane installation parameters on the obtained results is evident. In both examples and for both profile variants, the optimal width of the bottom flange corresponds to the minimum set value (b_m). For Example 2, for both variants, the optimal web height is equal to $h_m + 5 \text{ cm}$, which also represents a limit value (Tables 2 and 3). The optimal web thickness for both examples and both variants is the minimum set value (s), while the optimal weld size corresponds to the minimum set value a_w (Tables 2 and 3). Regarding the top flange thickness, for both examples in Variant 1, the minimum set value was obtained as optimal (t_2 , Table 2).

Tables 4 and 5 present the achieved and limit values of the constraint functions for both case studies (examples), for Variant 1 (Table 4) and Variant 2 (Table 5), respectively. These results clearly indicate which criteria are of primary importance for this type of carrying structure. As shown, weld stress and beam deflection have a negligible influence on the optimization results. The most critical criteria, with achieved values close to their permissible values, are the stability of the top flange and the stress at point C (bottom flange). This effect is particularly pronounced in Example 1, where the load capacity (Q) is significantly higher than in Example 2, while the mid-span between two supports (L) values are similar.

Table 4: Achieved and limit values for optimization constraints for Variant 1

Example	1		2	
	Constraint function	Achieved value	Limit (max/min) value	Achieved value
g_1 [kN/cm^2]	12.38	15.67	13.31	15.67
g_2 [kN/cm^2]	17.67	17.67	16.69	17.67
g_3 [kN/cm^2]	10.90	15.67	7.24	15.67
g_4 [kN/cm^2]	13.78	15.67	7.34	15.67
g_5 (cm)	0.36	0.70	0.29	0.86
g_6 [kN/cm^2]	13.78	15.24	7.34	12.96

Example	1	2	
g_7 [kN/cm ²]	13.78	13.78	7.34
g_8 [kN/cm ²]	2.74	11.75	1.16
g_9 (mm)	3	3.5	3
g_{10} (mm)	82	82	89
g_{11} (mm)	259.2	223	197

Table 5: Achieved and limit values for optimization constraints for Variant 2

Example	1	2		
Constraint function	Achieved value	Limit (max/min) value	Achieved value	Limit (max/min) value
g_1 [kN/cm ²]	12.45	15.67	13.30	15.67
g_2 [kN/cm ²]	17.67	17.67	16.65	17.67
g_3 [kN/cm ²]	10.90	15.67	7.19	15.67
g_4 [kN/cm ²]	10.90	15.67	7.19	15.67
g_5 (cm)	0.33	0.70	0.29	0.86
g_6 [kN/cm ²]	10.90	12.33	7.19	12.11
g_7 [kN/cm ²]	10.90	10.91	7.19	11.81
g_8 [kN/cm ²]	2.82	11.75	1.16	11.75
g_9 (mm)	3	3.5	3	3.5
g_{10} (mm)	82	82	89	89
g_{11} (mm)	241.4	223	197	197

5. CONCLUSION

This study focuses on the analysis and optimal design of a welded I-girder used in a monorail crane system. The objective function is defined as the minimization of mass, i.e., the cross-sectional area. The optimization variables include both the geometric dimensions of the I-section plates and the weld sizes. In addition to strength criteria at critical points of the I-section and welds, constraints related to stability, stiffness, and specific geometric limitations are also considered. An Evolutionary Algorithm (EA) implemented in MS Excel using the Solver add-in is applied as the optimization method, due to its capability to handle discrete values defined within predefined sets for the optimization variables. The optimization procedure is carried out on two monorail tracks currently in service (Table 1).

In this study, savings in the material are in the range of 42.61–54.03% for Variant 1 (the mono-symmetric I-profile, Table 2) and 42.02–48.78% for Variant 2 (the double-symmetric I-profile, Table 3). The results obtained in this research justify the approach for analysis and chosen optimization method for a welded I-girder of a monorail track. The influence of crane installation parameters on the obtained results is analyzed, as well as the effect of set minimum values on the optimal values of selected geometric parameters. The results indicate that certain criteria, such as weld stress and beam deflection, have a minor influence on the optimization outcome, whereas other criteria, including girder stability and stresses in the bottom flange plate, play a dominant role (Tables 4 and 5).

The proposed approach to analysis, design, and optimization using a MS Excel spreadsheet and an EA enables engineers and designers to efficiently obtain optimal solutions while maintaining full insight into constraint functions and all relevant design conditions. This methodology is not limited to carrying structures but can be applied to a wide range of engineering problems.

Future research should extend the analysis by considering the combination of different steel grades, material cost, and selected technological constraints in order to achieve solutions with minimal mass and overall cost of the monorail track girder. Additionally, the developed models should be verified using the Finite Element Method (FEM).

ACKNOWLEDGEMENTS

This work has been supported by the Ministry of Science, Technological Development and Innovation of the Republic of Serbia, through the Contracts for the scientific research financing in 2025, 451-03-137/2025-03/200108 and 451-03-136/2025-03/200108.

REFERENCES

- [1] K. M. Özdemir, "Lateral buckling of overhanging crane trolley monorails", *Engineering Structures*, Vol. 28(8), pp. 1129–1138, <https://doi.org/10.1016/j.engstruct.2005.12.006>, (2006)
- [2] N. S. Trahair, "Lateral buckling of monorail beams", *Engineering Structures*, Vol. 30(11), pp. 3213-3218, <https://doi.org/10.1016/j.engstruct.2008.05.001>, (2008)
- [3] N. S. Trahair, "Distortional buckling of overhanging monorails", *Engineering Structures*, Vol. 32(4), pp. 982–987, <https://doi.org/10.1016/j.engstruct.2009.12.025>, (2010)
- [4] S. Sagar, R. R. Patel and S. P. Joshi, "A literature review on design of overhead monorail crane for material handling", *International Journal for Scientific Research and Development*, Vol. 3(03), pp. 2621-2623, (2015)
- [5] A. Handoko, Y. R. Aldori, F. Farsa, N. A Setyanto and Masrajuddin, "Structural performance analysis of an 8-ton monorail crane using frame analysis and bolt connection evaluation", *IRA Journal of Mechanical Engineering and Applications*, Vol. 4(3), pp. 254-263, <https://doi.org/10.56862/irajtma.v4i3.359>, (2025)
- [6] G. Pavlović, B. Jerman, M. Savković, N. Zdravković and G. Marković, "Metaheuristic applications in mechanical and structural design", *Engineering Today*, Vol. 1(1), pp. 19-26, <https://doi.org/10.5937/engtoday2201019P>, (2022)
- [7] G. Pavlović, M. Savković, G. Marković and N. Zdravković, "Analysis of variants of structures of built-up columns on examples of columns for crane runways", *Proceedings of V Conference on Mechanical Engineering Technologies and Applications "COMETa 2020"*, Jahorina (B&H, Republic of Srpska), 26-28 November, pp. 235-242, (2020)
- [8] G. Pavlović, M. Savković, N. B. Zdravković, G. Marković, M. Todorović and P. Mladenović, "Optimal design of the hybrid i-girder of the single-beam bridge crane", *Proceedings of VII Conference on Mechanical Engineering Technologies and Applications "COMETa 2024"*, Jahorina (B&H, Republic of Srpska), 14-16 November, pp. 300-307, (2024)
- [9] Z. Petković and D. Ostrić, "Metalne konstrukcije u mašinogradnji I", University of Belgrade, Faculty of Mechanical Engineering, Belgrade (Serbia), (1996)
- [10] D. Ostrić and S. Tošić, "Dizalice", University of Belgrade, Faculty of Mechanical Engineering, Belgrade (Serbia), (2005)
- [11] SRPS U.E7.101:1991, Provera stabilnosti nosećih čeličnih konstrukcija - Bočno izvijanje nosača, Institute for Standardization of Serbia, Belgrade (Serbia), (1991)
- [12] SRPS U.E7.081:1986, Provera stabilnosti nosećih čeličnih konstrukcija - Centrično pritisnuti štapovi konstantnog jednodelnog preseka, Institute for Standardization of Serbia, Belgrade (Serbia), (1986)
- [13] SRPS U.E7.086:1986, Provera stabilnosti nosećih čeličnih konstrukcija - Određivanje dužine izvijanja štapova, Institute for Standardization of Serbia, Belgrade (Serbia), (1986)